

Understanding of collective atom phase control in modified photon echoes for near perfect retrieval efficiency in quantum memory

Rahmatullah^{1,2} and B. S. Ham^{1†}

¹Center for Photon Information Processing, and School of Electrical Engineering and Computer Science,
Gwangju Institute of Science and Technology, Gwangju, 61005 Republic of Korea

²Quantum Optics Lab., Department of Physics, COMSATS Institute of Information Technology, Islamabad, Pakistan

[†]Corresponding author: bham@gist.ac.kr

(March 10, 2017)

Abstract: Near perfect retrieval efficiency has been analyzed by solving the Maxwell–Bloch equations for multimode and storage time-extended quantum memory applications in a backward photon echo scheme. The backward photon echo scheme is combined with a controlled coherence conversion process via control Rabi flopping to a third state, where the controlled coherence conversion collectively shifts the ensemble’s phase for the photon echo and coherently determines the phase matching condition between the data (quantum) and the control (classical) pulses. Herein we discuss the classical controllability of a quantum state for both phase and propagation direction by using the control pulse areas in both single and double rephasing photon echo schemes in a three-level system. Compared with their well-understood use for two-level photon echoes, the Maxwell–Bloch equations to a three-level system have a critical limitation regarding the phase change when interacted with an arbitrary control pulse area.

Introduction

Over the last decade modified photon echo techniques have been intensively studied and applied to quantum memory to overcome the fundamental limitation of population inversion in conventional photon echoes, for which the population inversion excited by an optical π pulse results in quantum noises caused by spontaneous and/or stimulated emissions [1-17]. Although some of these techniques have been successful for quantum state storage and retrieval [8-13], the understanding of collective atom phase control has still been limited, resulting in ultralow echo efficiency owing to absorptive photon echoes such as in the techniques of controlled atomic frequency comb (AFC) echoes [8,9] and doubly rephased (DR) photon echoes [10-13]. To solve the absorptive photon echoes in the coherent transients of an ensemble, a controlled coherence conversion (CCC) process has been proposed [18] and experimentally demonstrated [19] for control of the ensemble phase, resulting in emissive photon echoes without population inversion. Recent observations of photon echoes in single [8,9] and double [10-13] rephasing photon echo schemes, however, appear to contradict the premise of the CCC protocol. Such an apparent contradiction between observation and theory has been analyzed and discussed for coherence leakage by the Gaussian spatial distribution of commercial laser light, resulting in 26% echo efficiency even for an unpermitted photon echo condition [20]. In addition to our previous studies on numerical [14-16] and analytical [17] approaches, herein we discuss the CCC theory by using the commonly applied Maxwell–Bloch approach to correct the critical mistakes of previous works [8-13] and thus to contribute to the development of photon echo–based quantum memory.

In the study of modified photon echoes for quantum memory, a common theoretical tool is to use the Maxwell–Bloch equations. These equations have the advantage of using both space and time variables, and thus are practical for calculations of photon echo efficiency in an actual medium with respect to its optical depth (or physical length) [1-4]. However, the Maxwell–Bloch approach is completely unable to give exact calculations of individual atom phase evolutions, making continuous tracing of ensemble coherence change in the time domain impossible. This limitation requires us to rely totally upon inevitable assumptions for the coherent transients in interactions with optical fields such as rephasing and control pulses, preventing us from obtaining exact answers to the phase change of the ensemble coherence with respect to the pulse area of an interacting optical field. To overcome this limitation of the Maxwell–Bloch approach, we have dealt with full numerical [14-16] and full analytical [17] solutions based on time-dependent density matrix equations to exactly trace the coherence evolutions of an ensemble. As a result, we have introduced the controlled double rephasing (CDR) echo protocol [14] based upon CCC [18]. Although CDR is perfect to investigate temporal coherence behaviors of coherent transient phenomena, such techniques of numerical and analytical calculations are limited in the calculations of optical depth-dependent photon echo efficiency. In the present report, we comply with the Maxwell–Bloch equations, firstly to confirm the CDR echo protocol with previous results of CCC in Refs. 17 and 18, secondly to analyze the critical mistakes in Refs. 8-13 arising from incorrect assumptions, and finally to discuss ensemble phase evolutions and their phase control in both single [8,9] and double rephasing schemes [10-14] for near perfect retrieval efficiency. Near perfect retrieval efficiency is critical for both fault-tolerant quantum computing [21] and

loophole-free quantum cryptography [22].

Theory: Maxwell–Bloch equations

A. Conventional two-pulse photon echo

We consider a three-level optical ensemble medium composed of N indistinguishable atoms. The energy level diagram and the pulse sequence of the present CDR echo scheme are depicted in Fig. 1. The data (D), the first rephasing (R_1) and the second rephasing (R_2) pulses are resonant to the transition of $|1\rangle - |2\rangle$ to satisfy the requirements of the double rephasing (DR) photon echo scheme [10-17]. The control pulses C_1 and C_2 are resonant between states $|2\rangle$ and $|3\rangle$ to enable CCC [14-19]. Initially all atoms of the medium are in the ground state, $|1\rangle$. For an ideal system, all decay rates are neglected unless specified otherwise. All light pulses are collinear (or near collinear) in the z -axis. To make the first echo (E_1) silent to avoid affecting the final echo (E_2), the rephasing pulse propagation directions are set to be opposite (backward) to that of the D pulse [10]. To satisfy the backward photon echo condition, the control pulses are set to be counter-propagating [19]: $\vec{k}_{E_2} = \vec{k}_{C_1} + \vec{k}_{C_2} - \vec{k}_D$; each pulse j is characterized by a wave vector \vec{k}_j . Unlike phase mismatching in silent echo (E_1) formation, which is determined by R_1 , the final echo (E_2) propagation direction (\vec{k}_{E_2}) is determined by the control pulse only [14]. The Maxwell–Bloch equations for the atomic coherence and the D pulse are respectively denoted by the following:

$$\frac{\partial}{\partial t} \sigma_{12}(z, t, \Delta) = i\Delta\sigma_{12}(z, t, \Delta) + i\varepsilon_D(z, t), \quad (1)$$

$$\frac{\partial}{\partial z} \varepsilon_D(z, t, \Delta) = \frac{i\alpha}{2\pi} \int_{-\infty}^{\infty} \sigma_{12}(z, t, \Delta) d\Delta, \quad (2)$$

where α is the optical depth parameter and Δ is the detuning of the atom (see Supplementary Information). The ensemble is inhomogeneously broadened by $\Delta' = \sum_j \Delta_j$. Here, we consider the case of a Δ -detuned atom for simplicity. Thus, the solution for atomic coherence is given by

$$\sigma_{12}(z, t, \Delta) = i \int_{-\infty}^t \varepsilon_D(z, \hat{t}) e^{i\Delta(t-\hat{t})} d\hat{t}. \quad (3)$$

The positive sign of this equation represents the fact that the atomic coherence excited by the D pulse is absorptive. It should be noted that $\sigma_{12}(z, t, \Delta) = -\rho_{12}(z, t, \Delta)$, where $\rho_{12}(z, t, \Delta)$ is the density matrix element. The solution of equation (2) gives the well-known Beer's law, namely $\varepsilon_D(z, t) = \varepsilon_D(0, t) e^{-\alpha z/2}$. The D pulse is assumed to be fully absorbed by the medium, thereby transferring its quantum information (phase, amplitude, polarization, etc.) into the collective atomic coherence. We assume that the D pulse is very weak to treat it as a quantum state. Thus, the ground state population change arising from the D pulse excitation is neglected: $\sigma_{11}(z, t, \Delta) = 1$.

With the time delay of T as shown in Fig. 1b, the rephasing pulse (R_1) arrives at $t = t_{R_1}$. The R_1 pulse has a π pulse area, and its propagation direction is opposite to that of the D pulse ($\vec{k}_{R_1} = -\vec{k}_D$). Here the function of the R_1 pulse is to swap the populations between states $|1\rangle$ and $|2\rangle$: $\sigma_{11}(z, t_D, \Delta) \xleftrightarrow{R_1} \sigma_{22}(z, t_{R_1}, \Delta)$. With the weak D pulse, the swapping result is $\sigma_{22}(z, t, \Delta) = 1$. Thus, the atomic coherence arising from the application of the R_1 pulse becomes

$$\frac{\partial}{\partial t} \sigma_{12}(z, t, \Delta) = i\Delta\sigma_{12}(z, t) - i\varepsilon_{R_1}(z, t). \quad (4)$$

The solution of equation (4) is

$$\sigma_{12}(z, t, \Delta) = e^{i\Delta(t-t_{R_1})} \sigma_{12}(z, t_{R_1}, \Delta) - i \int_{t_{R_1}}^t \varepsilon_{R_1}(z, \hat{t}) e^{i\Delta(t-\hat{t})} d\hat{t}. \quad (5)$$

Because the π pulse reverts the coherence evolution direction, $\sigma_{12}(z, t_{R_1}, \Delta)$ is equal to the conjugate of equation (3) at $t = t_{R_1}$, namely $\sigma_{12}(z, t_{R_1}, \Delta) = [\sigma_{12}(z, t = t_{R_1}, \Delta)]^\dagger$. Therefore, equation (5) can be rewritten as

$$\sigma_{12}(z, t, \Delta) = -i e^{-i\Delta(2t_{R_1}-t)} \int_{-\infty}^{\infty} \varepsilon_D^\dagger(z, \hat{t}) e^{i\Delta\hat{t}} d\hat{t} - i \int_{t_{R_1}}^t \varepsilon_{R_1}(z, \hat{t}) e^{i\Delta(t-\hat{t})} d\hat{t}, \quad (6)$$

where the first term represents free evolution and the second term represents interaction with the rephasing pulse. The ensemble coherence generated by the D pulse becomes in phase and results in a photon echo E_1 at $t = t_{E_1} = 2t_{R_1} - t_D$. The propagation direction of the first echo E_1 determined by the first rephasing pulse R_1 is $\vec{k}_{E_1} = 2\vec{k}_{R_1} - \vec{k}_D = -3\vec{k}_D$. Due to the phase mismatch between D and E_1 , the echo signal (macroscopic coherence) is not inphase [10]: Silent echo.

B. DR echo

To rephase the system one more time, the second rephasing (R_2) π pulse is followed by E_1 to satisfy the requirements of the DR photon echo scheme. In the DR scheme, the excited state population after the final echo E_2 is the same as that after the D pulse excitation. This means that all excited-state atoms in the DR scheme should contribute to the echo signal without contributing to quantum noise. The Maxwell–Bloch equation for DR is similar to the equations for D, and the optical coherence solution for the final echo E_2 is

$$\sigma_{12}(z, t, \Delta) = e^{i\Delta(t-t_{R_2})} \sigma_{12}(z, t_{R_2}, \Delta) + i \int_{t_{R_2}}^t \varepsilon_{R_2}(z, \hat{t}) e^{i\Delta(t-\hat{t})} d\hat{t}, \quad (7)$$

where $\sigma_{12}(z, t_{R_2}, \Delta)$ is equal to the conjugate of equation (6) at $t = t_{R_2}$:

$$\begin{aligned} \sigma_{12}(z, t, \Delta) = & i e^{-i\Delta(2t_{R_2}-2t_{R_1}-t)} \int_{-\infty}^{\infty} \varepsilon_D(z, \hat{t}) e^{-i\Delta\hat{t}} d\hat{t} + i e^{-2i\Delta t_{R_2}} \int_{-\infty}^{\infty} \varepsilon_{t_{R_1}}^\dagger(z, \hat{t}) e^{i\Delta(t+\hat{t})} d\hat{t} \\ & + i \int_{t_{R_2}}^t \varepsilon_{R_2}(z, \hat{t}) e^{i\Delta(t-\hat{t})} d\hat{t}. \end{aligned} \quad (8)$$

The final echo E_2 is formed at $t = t_{E_2}$ as the rephasing result of E_1 , and its propagation direction is forward if $\vec{k}_{R_2} = \vec{k}_{R_1}$: $\vec{k}_{E_2} = 2\vec{k}_{R_2} - \vec{k}_{E_1} = 2\vec{k}_{R_2} - (2\vec{k}_{R_1} - \vec{k}_D) = \vec{k}_D$. However, the retrieved signal E_2 is absorbed by the medium due to absorptive coherence as shown in equation (8). In other words, echo E_2 cannot be radiated from the medium. This fact has already been explored numerically [14-16] and analytically [17]. From now on we discuss and correct critical mistakes in previous analyses [8-13]. By the way, the observation of DR echoes [10-13] has been understood as a coherence leakage due to an imperfect rephasing process by Gaussian-distributed light in a transverse mode, resulting in the leakage-caused maximum retrieval efficiency reaches at 26% [20].

Discussion

A. CDR echo

To fix the absorptive echo problem in DR, the CDR echo protocol has been proposed whereby the control pulse pair C_1 and C_2 are added as shown in Fig. 1b [14]. As discussed in Refs. [14-18], the function of the control pulses is not only to convert the coherence between optical and spin states via population transfer, but also to induce a collective phase shift. Moreover, unlike the DR scheme of equation (8), the propagation vector of E_2 can be controlled to be backward if $\vec{k}_{C_1} = -\vec{k}_{C_2}$: $\vec{k}_{E_2} = \vec{k}_{C_1} + \vec{k}_{C_2} - \vec{k}_D = -\vec{k}_D$ [14,19]. Here, the rephasing pulses have nothing to do with determining \vec{k}_{E_2} . Unlike the forward echo in the conventional two-pulse photon echo scheme, which suffers from reabsorption by noninteracting atoms according to Beer's law, the backward echo E_2 is free from reabsorption, resulting in near perfect echo efficiency [1,2,19]. To eliminate any potential two-photon coherence between states $|1\rangle$ and $|3\rangle$, the C_1 pulse is delayed by δT from R_1 . Here, it should be noted that the *macroscopic* two-photon coherence is sustained only within the overall optical coherence time determined by the inverse of the atom broadening Δ' . However, *individual* atom coherence is sustained regardless of broadening for the optical phase decay time T_2 , where $T_2 \gg \Delta T$ [18]. Here the D pulse duration is practically comparable to (or a bit longer than) $1/\Delta'$. Thus, by simply neglecting δT , the atomic coherence at t_{C_1} can be expressed as

$$\sigma_{12}(z, t_{C_1}, \Delta) = i e^{-i\Delta(2t_{R_2}-2t_{R_1}-t_{C_1})} \int_{-\infty}^{\infty} \varepsilon_D(z, \hat{t}) e^{-i\Delta \hat{t}} d\hat{t}. \quad (9)$$

In equation (9) we have only considered the first term of equation (8), which is related to the free evolution of the coherences generated by the D pulse; the second and third terms are associated with the rephasing fields. Because the first echo E_1 is silent, and the second echo E_2 is not emitted owing to its absorptive coherence, we can remove the last two terms of equation (8). With a π C_1 pulse, optical and spin coherence respectively satisfy the following relations: $\sigma_{12}(z, t, \Delta) = \cos\left(\frac{\pi}{2}\right) \sigma_{12}(z, t_{C_1}, \Delta) = 0$; $\sigma_{13}(z, t, \Delta) = e^{i\pi/2} \sigma_{12}(z, t_{C_1}, \Delta)$ (see Refs. 14-18). The C_1 pulse induces a $\pi/2$ phase shift and locks the optical coherence until C_2 arrives. Here, the novel property of the $\pi/2$ phase shift from the π pulse area of C_1 (or C_2) originates in the Raman (two-photon) coherence, where a 2π Raman pulse in a three-level system actually acts as a π pulse does in a two-level system: see Figs. 3 and 4 of Ref. [23] and Fig. 4 of Ref. [24]. There is no way to expect this novel property from the Maxell–Bloch approach. Without a priori understanding of the coherence behavior in a three-level system, the same mistake has been repeated in the controlled AFC echoes [8,9]; this will be discussed further in section B.

The atomic coherence after the C_2 pulse is

$$\frac{\partial}{\partial t} \sigma_{12}(z, t, \Delta) = i\Delta \sigma_{12}(z, t, \Delta). \quad (10)$$

Equation (10) is obtained by substituting $\varepsilon_i = 0$ and $\sigma_{13}(z, t, \Delta) = 0$ (no spin coherence after C_2) into equation (S4) of the Supplementary Information. The solution of equation (10) is

$$\sigma_{12}(z, t, \Delta) = \sigma_{12}(z, t_{C_2}, \Delta) e^{i\Delta(t-t_{C_2})}. \quad (11)$$

The C_2 pulse also brings a $\pi/2$ phase shift while swapping the spin and optical coherence:

$$\sigma_{12}(z, t_{C_2}, \Delta) = e^{i\pi/2} \sigma_{13}(z, t, \Delta) = e^{i\pi} \sigma_{12}(z, t_{C_1}, \Delta) = -i e^{-i\Delta(2t_{R_2}-2t_{R_1}-t_{C_1})} \int_{-\infty}^{\infty} \varepsilon_D(z, \hat{t}) e^{-i\Delta \hat{t}} d\hat{t}. \quad (12)$$

Substituting equation (12) into equation (11) gives

$$\begin{aligned} & \sigma_{12}(z, t, \Delta) \\ &= -i e^{-i\Delta(t_{C_2}-t_{C_1}+2t_{R_2}-2t_{R_1}-t)} \int_{-\infty}^{\infty} \varepsilon_D(z, \hat{t}) e^{-i\Delta \hat{t}} d\hat{t}; \end{aligned} \quad (13)$$

the negative sign of this equation represents the fact that the echo E_2 is emissive due to the π phase shift induced by the control pulse pair, which has already been extensively explored numerically [14-16] and analytically [17]. Thus, the echo E_2 propagates backward without reabsorption and is radiated out of the medium with near perfect retrieval efficiency; this will be discussed further in Fig. 2.

B. Single rephased photon echo

Now we consider the coherence evolution for a controlled single rephasing scheme with $R_2=0$ (Fig. 1) [18,19]. This scheme itself cannot be used for quantum memory because the population inversion has not been solved yet. However, it also implies AFC echoes, whereby all excited-state atoms freely decay into a dump state. The AFC scheme can be easily obtained by swapping the pulse sequences of D and R_1 , and substituting R_1 with a repeated weak two-pulse train (see Supplementary Information). So, neglecting the population constraint issue without R_2 as shown in Fig. 1, the final optical coherence can be obtained by applying the control pulses to equation (6) (see Section III of the Supplementary information) as follows:

$$\sigma_{12}(z, t, \Delta) = i e^{-i\Delta(t_{C_2}-t_{C_1}+2t_{R_1}-t)} \int_{-\infty}^{\infty} \varepsilon_D^\dagger(z, \hat{t}) e^{i\Delta \hat{t}} d\hat{t}. \quad (14)$$

The positive sign of this equation represents the absorptive coherence, which is the same problem as in the DR scheme in equation (8). In other words, the π - π control pulse sequence added to the single rephasing scheme inverts

the system coherence to be absorptive [18]. To convert the absorptive echo into an emissive one, simply one more control Rabi flopping is added, for which the C_2 pulse area is increased to 3π ; i.e., $\sigma_{12}(z, t, \Delta) \xrightarrow{C_1(\pi)} e^{-\left(\frac{\pi}{2}\right)i} \sigma_{13}(z, t, \Delta) \xrightarrow{C_2(\pi)} e^{\pi i} \sigma_{12}(z, t, \Delta) \xrightarrow{C_2(2\pi)} e^{-\left(\frac{3\pi}{2}\right)i} \sigma_{13}(z, t, \Delta) \xrightarrow{C_2(3\pi)} e^{2\pi i} \sigma_{12}(z, t, \Delta)$, and $\sigma_{12}(z, t, \Delta)$ is negative. This means that the π - π control pulse sequence in Refs. [8] and [9] must be corrected to be a π - 3π control pulse sequence. Here, the π - π control pulse sequence in Ref. [1] is using a Doppler effect-caused π -phase shift, resulting in an emissive echo. This is not the case for a solid medium [2,14,18]. The observation of controlled AFC echoes with a π - π control pulse set [8,9] has been understood to arise from the imperfect rephasing by commercial light sources with Gaussian spatial distributions [20]. The coherence leakage induced by the Gaussian pulse limits the echo efficiency to $\sim 10\%$ on average regardless of the rephasing pulse area, whereas its maximum efficiency reaches 26% for a $\pi/2$ pulse area [20].

C. Near perfect retrieval efficiency in CDR

We now calculate the echo efficiency of the present CDR echo scheme shown in Fig. 1. Because the echo E_2 is emitted in the backward direction, the atomic coherence and optical field in the backward direction can be respectively represented as follows [25]:

$$\frac{\partial}{\partial t} [\sigma_{12}(z, t, \Delta)]_b = i\Delta [\sigma_{12}(z, t, \Delta)]_b + i\varepsilon_b(z, t), \quad (15)$$

$$\frac{\partial}{\partial z} \varepsilon_b(z, t) = -\frac{i\alpha}{2\pi} \int_{-\infty}^{\infty} [\sigma_{12}(z, t, \Delta)]_b d\Delta. \quad (16)$$

The solution of equation (15) is

$$[\sigma_{12}(z, t, \Delta)]_b = [\sigma_{12}(z, 0, \Delta)]_b e^{i\Delta t} + i \int_0^t \varepsilon_b(z, \acute{t}) e^{i\Delta(t-\acute{t})} d\acute{t}, \quad (17)$$

where $[\sigma_{12}(z, 0, \Delta)]_b$ is obtained by setting $t = 0$ in equation (13).

$$[\sigma_{12}(z, 0, \Delta)]_b = \sigma_{12}(z, t = 0, \Delta) = -i e^{-i\Delta(t_{C_2} - t_{C_1} + 2t_{R_2} - 2t_{R_1})} \int_{-\infty}^{\infty} \varepsilon_D(z, \acute{t}) e^{-i\Delta \acute{t}} d\acute{t}. \quad (18)$$

Inserting equation (18) into equation (17) gives

$$[\sigma_{12}(z, t, \Delta)]_b = -i e^{-i\Delta(t_{C_2} - t_{C_1} + 2t_{R_2} - 2t_{R_1} - t)} \int_{-\infty}^{\infty} \varepsilon_D(z, \acute{t}) e^{-i\Delta \acute{t}} d\acute{t} + i \int_0^t \varepsilon_b(z, \acute{t}) e^{i\Delta(t-\acute{t})} d\acute{t}. \quad (19)$$

Equations (19) and (16) are solved by means of Laplace transformation. For the backward scheme, $\varepsilon_b(L, \omega) = 0$ because there is no field at $z = L$. Assuming an ideal case of complete absorption at $z = L$, solving equations (19) and (16) yields

$$\varepsilon_b(0, \omega) = (1 - e^{-\alpha L}) e^{-i\omega(t_{C_2} - t_{C_1} + 2t_{R_2} - 2t_{R_1} - t_D)} \varepsilon_D(0, \omega). \quad (20)$$

The inverse Fourier transform gives

$$\varepsilon_b(0, t) = (1 - e^{-\alpha L}) \varepsilon_D(0, t - (t_{C_2} - t_{C_1} + 2(t_{R_2} - t_{R_1}))), \quad (21)$$

where the echo is emitted at $t = t_{E_2} = t_{C_2} - t_{C_1} + 2(t_{R_2} - t_{R_1}) + t_D$. Because $t_{C_2} - t_{C_1}$ can be lengthened to be much longer than $t_{R_1} - t_D$ in a Zeeman scheme, an additional but important function of the control pulse set is storage time extension [8,9,19]. The efficiency of the final backward echo E_2 is given by

$$\eta = (1 - e^{-\alpha L})^2, \quad (22)$$

where η can be near unity in an optically dense medium as shown in Fig. 2.

On the other hand, the forward echo E_2 can be obtained by setting $\vec{k}_{C_1} = \vec{k}_{C_2}$, where $\vec{k}_{C_1} = \vec{k}_D$: $\vec{k}_{E_2} = \vec{k}_{C_1} + \vec{k}_{C_2} - \vec{k}_D = 2\vec{k}_{C_1} - \vec{k}_D = \vec{k}_D$. Here, the difference frequency between C_1 and D is just ~ 10 MHz, about 10^{-8} times the frequency of visible light. The atomic coherence and the forward field satisfy the following relations:

$$\frac{\partial}{\partial t} [\sigma_{12}(z, t, \Delta)]_f = i\Delta [\sigma_{12}(z, t, \Delta)]_f + i\varepsilon_f(z, t), \quad (23)$$

$$\frac{\partial}{\partial z} \varepsilon_f(z, t) = \frac{i\alpha}{2\pi} \int_{-\infty}^{\infty} [\sigma_{12}(z, t, \Delta)]_f d\Delta. \quad (24)$$

By following the same procedure as used for backward echo above, the optical field propagating in the forward direction can be expressed as follows:

$$\varepsilon_f(L, t) = \alpha L e^{-\frac{\alpha L}{2}} \varepsilon_D(0, t - (t_{C_2} - t_{C_1} + 2(t_{R_2} - t_{R_1}))). \quad (25)$$

Thus, the retrieval efficiency of the forward echo E_2 is $(\alpha L)^2 e^{-\alpha L}$ (see the dotted curve in Fig. 2). Obviously the forward echo E_2 suffers from reabsorption.

In Fig. 2, we plot the echo efficiency of both the forward (dotted) and backward (solid) echo schemes for Fig. 1. For the forward echo, the retrieval efficiency reaches 54% at maximum, and then exponentially decreases due to the reabsorption process. On the other hand, the echo efficiency for the backward scheme approaches unity for $\alpha L \gg 0$ as expected according to Ref. 1 and demonstrated in Ref. 19.

Conclusions

Herein we have analyzed and discussed the modified photon echo schemes of controlled double rephasing (CDR) for near perfect echo efficiency with no population inversion. We also pointed out the absorptive echo problems in previously demonstrated single (AFC) and double rephasing photon echo schemes, where the mistake in the controlled AFC echoes arises from a wrong assumption applied to the Maxwell–Bloch approach for a three-level system: compared with a two-level system whose coherence harmonic is 2π -based, the three-level system shows 4π -based coherence harmonics. The Maxwell–Bloch method never gives an exact solution to the phase change of the ensemble coherence in its interaction with an arbitrary optical pulse area, unless known a priori as in the two-level system. With the help of full numerical [14-16] and analytic [17] calculations using density matrix equations, our present Maxwell–Bloch calculation results confirmed the CDR echo theory. Thus, the present report gives a clear understanding of collective atom phase control in modified photon echoes for quantum memory applications. The controlled coherence conversion process via control Rabi flopping to a third state was also investigated as a means of coherence inversion in a solid medium, whereby the absorptive coherence of the photon echo in the double rephasing scheme was converted into an emissive one. Finally, we discussed the near perfect CDR echo efficiency of a backward scheme using counter-propagating control Rabi pulses.

References

1. Moiseev, S. A. and Kröll, S. complete reconstruction of the quantum state of a single-photon wave packet absorbed by a Doppler-broadened transition. *Phys. Rev. Lett.* **87**, 173601 (2001).
2. Moiseev, S. A. Tarasov, V. F. and Ham, B. S. Quantum memory photon echo-like techniques in solids. *J. Opt. B: Quantum semiclass. Opt.* **5**, S497-S502 (2003).
3. Kraus, B, *et al.* Quantum memory for nonstationary light fields based on controlled reversible inhomogeneous broadening. *Phys. Rev. A* **73**, 020302 (2006).
4. Alexander, A. L. Longdell, J. J. Sellars, M. J. and Manson, N. B. Photon echoes produced by switching electric fields. *Phys. Rev. Lett.* **96**, 043602 (2006).
5. Hedges, M. P. Longdell, J. J. Li, Y. and Sellars, M. J. Efficient quantum memory for light. *Nature* **465**, 1052-1056 (2010).
6. Riedmatten, H. de *et al.* A solid-state light-matter interface at the single-photon level. *Nature* **456**, 773-777 (2008).
7. Saglamyurek, E. et al., Broadband waveguide quantum memory for entangled photons. *Nature* **469**, 512-515 (2011).
8. Afzelius, M. *et al.* Demonstration of atomic frequency comb memory for light with spin-wave storage. *Phys. Rev. Lett.* **104**, 040503 (2010).
9. Gündoğan, M. *et al.*, Coherent storage of temporally multimode light using a spin-wave atomic frequency comb memory. *New J. Phys.* **15**, 045012 (2013).
10. Damon, V. et al., Revival of silenced echo and quantum memory for light. *New J. Phys.* **13**, 093031 (2011).
11. Dajczgewand, J. *et al.*, Optical memory bandwidth and multiplexing capacity in the erbium telecommunication window. *New J. Phys.* **17**, 023031 (2015).
12. Arcangeli, A. Ferrier, A. and Goldner, Ph. Stark echo modulation for quantum memories. *Phys. Rev. A* **93**, 062303 (2016).
13. McAuslan, D. L. et al., Photon-echo quantum memories in inhomogeneously broadened two-level atoms. *Phys. Rev. A* **84**, 022309 (2011).
14. Ham, B. S. Atom phase controlled noise-free photon echoes. *arXiv:1101.5480v2* (2011).
15. Ham, B. S. Coherent control of collective atom phase for ultralong, inversion-free photon echoes. *Phys. Rev. A* **85**, 031402(R) (2012); *ibid*, *Phys. Rev. A* **94**, 049905(E) (2016).
16. Ham, B. S. A controlled ac Stark echo for quantum memories. Scientific Reports (To be published), *arXiv:1612.02193* (2016).
17. Rahmatullah and Ham, B. S. “Analysis of Controlled Coherence Conversion in a Double Rephasing Scheme of Photon Echoes for Quantum Memories. *arXiv: 1612.02167v2* (2016).
18. Ham, B. S. Control of photon storage time using phase locking. *Opt. Exp.* **18**, 1704 (2010).
19. Hahn, J. and Ham, B. S. Rephasing halted photon echoes using controlled optical deshelving. *New J. Phys.* **13**, 093011 (2011).
20. Ham, B. S. Gaussian beam profile effectiveness on double rephasing photon echoes. *arXiv:1701.04291* (2017).
21. Steane, A. M. Efficient fault-tolerant quantum computing. *Nature* **399**, 124 (1999).
22. Lo, H.-K. Curty, M. and Qi, B. Measurement-Device-Independent Quantum Key Distribution. *Phys. Rev. Lett.* **108**, 130503 (2012).
23. Ham, B. S. “Collective atom phase controls in photon echoes for quantum memory applications I: population inversion removal,” *arXiv:1612.00115* (2016).
24. Ham, B. S., Shahriar, M. S., Kim, M. K., and Hemmer, P. R. Spin coherence excitation and rephasing with optically shelved atoms. *Phys. Rev. B* **58**, R11825 (1998).
25. Sangouard, N. Simon, C. Afzelius, M. and Gisin, N. Analysis of a quantum memory for photons based on controlled reversible inhomogeneous broadening. *Phys. Rev. A* **75**, 032327 (2007).

Acknowledgment

The present work was supported by the ICT R&D program of MSIP/IITP (1711028311: Reliable crypto-system standards and core technology development for secure quantum key distribution network).

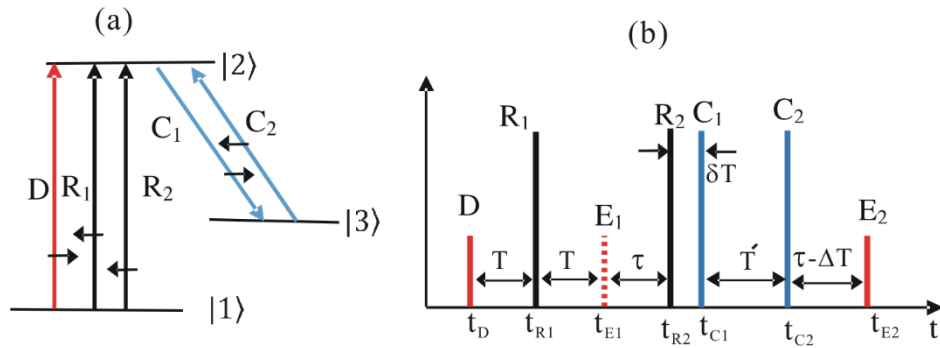


Figure 1. Schematics of controlled double rephasing (CDR) echoes. (a) Energy level diagram. The short black arrows indicate the pulse propagation direction. (b) Pulse sequence for (a). t_j is the arrival time of pulse j .

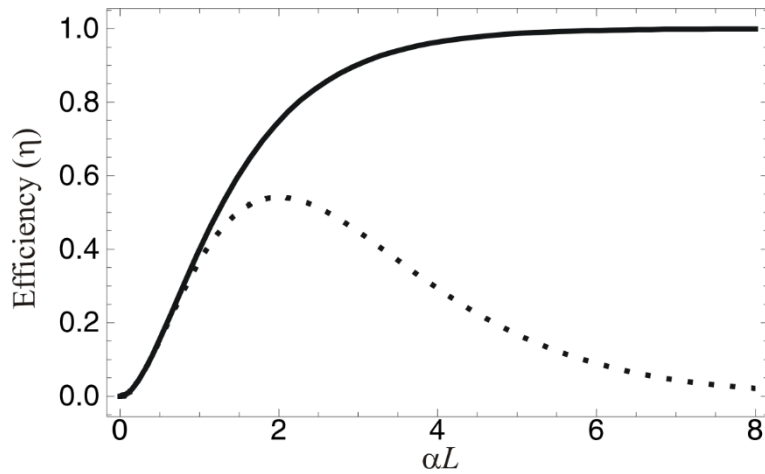


Figure 2. Efficiency of CDR echoes versus optical depth αL . The solid curve is for the backward echo E_2 ; see Eq. (16). The dotted curve is for the forward echo E_2 : $(\alpha L)^2 e^{-\alpha L}$.

Supplemental Information for “Controlled Double Rephasing Photon Echoes for Quantum Memories”

In Fig. S1(a), the D and R₁ pulses are resonant to the transition of $|1\rangle - |2\rangle$. The two counter-propagating C₁ and C₂ control pulses are resonant to the transition of $|2\rangle - |3\rangle$. The optical Bloch and the Maxwell-Schrödinger equations are:

$$\frac{\partial}{\partial t} \sigma_{11}(z, t, \Delta) = i\varepsilon_l(z, t)(\sigma_{12}(z, t, \Delta) - \sigma_{21}(z, t, \Delta)), \quad (S1)$$

$$\frac{\partial}{\partial t} \sigma_{22}(z, t, \Delta) = i\varepsilon_l(z, t)(\sigma_{21}(z, t, \Delta) - \sigma_{12}(z, t, \Delta)) + i\varepsilon_j(\sigma_{23}(z, t, \Delta) - \sigma_{32}(z, t, \Delta)), \quad (S2)$$

$$\frac{\partial}{\partial t} \sigma_{33}(z, t, \Delta) = i\varepsilon_j(\sigma_{32}(z, t, \Delta) - \sigma_{23}(z, t, \Delta)), \quad (S3)$$

$$\frac{\partial}{\partial t} \sigma_{12}(z, t, \Delta) = i\Delta\sigma_{12}(z, t, \Delta) + i\varepsilon_l(z, t)(\sigma_{11}(z, t, \Delta) - \sigma_{22}(z, t, \Delta)) + i\varepsilon_j(z, t)\sigma_{13}(z, t, \Delta), \quad (S4)$$

$$\frac{\partial}{\partial t} \sigma_{32}(z, t, \Delta) = i\Delta\sigma_{32}(z, t, \Delta) + i\varepsilon_j(z, t)(\sigma_{33}(z, t, \Delta) - \sigma_{22}(z, t, \Delta)) + i\varepsilon_l(z, t)\sigma_{31}(z, t, \Delta), \quad (S5)$$

$$\frac{\partial}{\partial t} \sigma_{13}(z, t, \Delta) = i\varepsilon_j(z, t)\sigma_{12}(z, t, \Delta) + i\varepsilon_l\sigma_{23}(z, t, \Delta), \quad (S6)$$

$$\frac{\partial}{\partial z} \varepsilon_{l(j)}(z, t) = \frac{i\alpha}{2\pi} \int_{-\infty}^{\infty} \sigma_{12}(z, t, \Delta) d\Delta, \quad (S7)$$

where, $l = D$ or R_1 and $j = C_1$ or C_2 . The $\varepsilon_{l(j)}$ is the optical field, α is the optical depth parameter, and $\Delta = \omega_{12} - \omega_l = \omega_{23} - \omega_j$ is the detuning of the atom. For the controlled single rephasing photon echo scheme without R₂, the controlled coherence conversion is studied below as discussed numerically [18] and experimentally [19]. The pulse sequence is shown in Fig. S1(b). This scheme itself is of course not suitable for quantum memory applications due to the unsolved π -pulse induced population inversion. However, in a modified photon echo scheme of atomic frequency comb (AFC) with repeated weak two-pulse train [6], the excited state population can be removed via spontaneous emission decay process onto a dump state such as in a persistent spectral hole burning rare-earth doped medium [24]. We have numerically analyzed that AFC belongs to the category of three-pulse photon echoes [25]. Either two-pulse or three pulse photon echoes, the rephased coherence of the ensemble is described in the same way. Thus, Fig. S1 is understood as a simple model for the quantum memory without losing generality if we neglect the population on the excited state.

I. D-pulse

A weak D-pulse propagates through the medium along z-direction. We assume that D-pulse is much weaker than the π -pulse and neglect population change by D: $\sigma_{11}(z, t, \Delta) = 1$. The resultant Maxwell-Bloch equations by D are obtained by substituting $\varepsilon_l = \varepsilon_D$ and $\varepsilon_j = 0$ in equations (S4) and (S7):

$$\frac{\partial}{\partial t} \sigma_{12}(z, t, \Delta) = i\Delta\sigma_{12}(z, t, \Delta) + i\varepsilon_D(z, t), \quad (S8)$$

$$\frac{\partial}{\partial z} \varepsilon_D(z, t) = \frac{i\alpha}{2\pi} \int_{-\infty}^{\infty} \sigma_{12}(z, t, \Delta) d\Delta. \quad (S9)$$

By applying an integrating factor $e^{-i\Delta t}$ to equation (S8), the solution is obtained:

$$\sigma_{12}(z, t, \Delta) = \sigma_{12}(z, -\infty, \Delta) + i \int_{-\infty}^t \varepsilon_D(z, \hat{t}) e^{i\Delta(t-\hat{t})} d\hat{t}. \quad (S10)$$

By setting the initial atomic coherence to be zero, $\sigma_{12}(z, -\infty, \Delta) = 0$:

$$\sigma_{12}(z, t, \Delta) = i \int_{-\infty}^t \varepsilon_D(z, \hat{t}) e^{i\Delta(t-\hat{t})} d\hat{t}. \quad (S11)$$

Here, the coherence is positive (absorptive). It should be noted that $\sigma_{12}(z, t, \Delta) = -\rho_{12}(z, t, \Delta)$, where $\rho_{12}(z, t, \Delta)$ is the density matrix element. Taking the Fourier transform of equation (S11) and substituting it into the Fourier version of (S9), we obtain:

$$\frac{\partial}{\partial z} \varepsilon_D(z, t) = -\frac{\alpha}{2\pi} \int_{-\infty}^{\infty} \varepsilon_D(z, \omega) \left[\frac{1}{i(\omega - \Delta)} + \pi(\omega - \Delta) \right] d\Delta = -\frac{\alpha}{2} \varepsilon_D(z, \omega). \quad (\text{S12})$$

The solution of equation (S12) in time domain is:

$$\varepsilon_D(z, t) = e^{-\frac{\alpha z}{2}} \varepsilon_D(0, t). \quad (\text{S13})$$

The D-pulse exponentially decays as it propagates through the medium: Beer's law.

II. R₁-pulse

To retrieve D pulse excited coherence, we apply a π R₁-pulse in delay time T after the D-pulse. By the R₁-pulse the atoms are excited ($\sigma_{22}(z, t, \Delta) = 1$), and the corresponding equations of motion are:

$$\frac{\partial}{\partial t} \sigma_{12}(z, t, \Delta) = i\Delta \sigma_{12}(z, t, \Delta) - i\varepsilon_{R_1}(z, t), \quad (\text{S14})$$

$$\frac{\partial}{\partial z} \varepsilon_{R_1}(z, t) = \frac{i\alpha}{2\pi} \int_{-\infty}^{\infty} \sigma_{12}(z, t, \Delta) d\Delta. \quad (\text{S15})$$

The equations (S14) and (S15) are obtained by substituting $\varepsilon_l = \varepsilon_{R_1}$ and $\varepsilon_j = 0$ into equations (S4) and (S7). The solution of equation (S14) yields:

$$\sigma_{12}(z, t, \Delta) = e^{i\Delta(t-t_{R_1})} \sigma_{12}(z, t_{R_1}, \Delta) - i \int_{t_{R_1}}^t \varepsilon_{R_1}(z, \acute{t}) e^{i\Delta(t-\acute{t})} d\acute{t}. \quad (\text{S16})$$

The R₁-pulse results in a phase conjugate of the D-excited coherence according to the photon echo theory, so the coherence at $t = t_{R_1}$ is equal to the conjugate of equation (S11):

$$\sigma_{12}(z, t, \Delta) = -i e^{-i\Delta(2t_{R_1}-t)} \int_{-\infty}^{\infty} \varepsilon_D^\dagger(z, \acute{t}) e^{i\Delta \acute{t}} d\acute{t} - i \int_{t_{R_1}}^t \varepsilon_{R_1}(z, \acute{t}) e^{i\Delta(t-\acute{t})} d\acute{t}. \quad (\text{S17})$$

The negative sign in equation (S17) shows the emissive coherence of the photon echo. With some mathematical calculations, we obtain the following equation in a frequency domain:

$$\sigma_{12}(z, \omega, \Delta) = -i e^{-2i\Delta t_{R_1}} 2\pi \delta(\omega - \Delta) \int_{-\infty}^{\infty} \varepsilon_D^\dagger(z, \acute{t}) e^{i\Delta \acute{t}} d\acute{t} - i \varepsilon_{R_1}(z, \omega) \left[\frac{1}{i(\omega - \Delta)} + \pi \delta(\omega - \Delta) \right]. \quad (\text{S18})$$

By taking the Fourier transform of equation (S15) and substituting with equation (S18), we get:

$$\varepsilon_{R_1}(z, t) = \varepsilon_{R_1}(0, t) e^{\frac{\alpha z}{2}} + 2 \sinh\left(\frac{\alpha z}{2}\right) \varepsilon_D^\dagger(0, 2t_{R_1} - t). \quad (\text{S19})$$

The echo is emitted at $t = 2t_{R_1} - t_D$. The efficiency of the echo is $4\sinh^2\left(\frac{\alpha z}{2}\right)$, which is greater than unity for a large optical depth due to the stimulated emission in the inverted medium [26,27]. However, as mentioned earlier, there is no amplification if there is no population inversion like AFC.

III. C_1 and C_2 -pulses

The function of C_1 -pulse is to convert the optical coherence $\sigma_{12}(z, t, \Delta)$ into spin coherence $\sigma_{13}(z, t, \Delta)$. The coherence at t_{C_1} is given by:

$$\sigma_{12}(z, t, \Delta) = -i e^{-i\Delta(2t_{R_1}-t_{C_1})} \int_{-\infty}^{\infty} \varepsilon_D^\dagger(z, \hat{t}) e^{i\Delta \hat{t}} d\hat{t}. \quad (S20)$$

Here, the first term of equation (S17) related to the evolution of the coherences excited by the D-pulse. The optical coherence is transferred to spin coherence: $\sigma_{12}(z, t, \Delta) = \cos\left(\frac{\pi}{2}\right) \sigma_{12}(z, t_{C_1}, \Delta) = 0$; $\sigma_{13}(z, t, \Delta) = e^{i\pi/2} \sigma_{12}(z, t_{C_1}, \Delta)$ [17,18]. The πC_1 -pulse incurs an additional $\pi/2$ phase shift, resulting in freezing optical coherence evolutions. The C_2 -pulse transfers the spin coherence back into the optical coherence. By setting $\varepsilon_l = 0$ and $\sigma_{13}(z, t, \Delta) = 0$ in equation (S4), we get:

$$\frac{\partial}{\partial t} \sigma_{12}(z, t, \Delta) = i\Delta \sigma_{12}(z, t, \Delta). \quad (S21)$$

The solution of (S21) is:

$$\sigma_{12}(z, t, \Delta) = \sigma_{12}(z, t_{C_2}, \Delta) e^{i\Delta(t-t_{C_2})}, \quad (S22)$$

The πC_2 -pulse reswaps the coherences with another $\pi/2$ phase shift:

$$\sigma_{12}(z, t_{C_2}, \Delta) = e^{i\pi/2} \sigma_{13}(z, t, \Delta) = e^{i\pi} \sigma_{12}(z, t_{C_1}, \Delta) = i e^{-i\Delta(2t_{R_1}-t_{C_1})} \int_{-\infty}^{\infty} \varepsilon_D^\dagger(z, \hat{t}) e^{i\Delta \hat{t}} d\hat{t}. \quad (S23)$$

Substituting equation (S23) into (S22), we obtain:

$$\sigma_{12}(z, t, \Delta) = i e^{-i\Delta(t_{C_2}-t_{C_1}+2t_{R_1}-t)} \int_{-\infty}^{\infty} \varepsilon_D^\dagger(z, \hat{t}) e^{i\Delta \hat{t}} d\hat{t}. \quad (S24)$$

Here the final atomic coherence is positive. Thus, the echo becomes absorptive and cannot be radiated from the medium [18]. If the area of the C_2 is 2π , it brings the atomic coherence halted ($\sigma_{12}(z, t) = 0$) again transferring it to the spin state $|3\rangle$. For a 3π - C_2 , the atoms are returned to the excited state $|2\rangle$, and $\sigma_{12}(z, t_{C_2}t_{C_2}, \Delta) = -\sigma_{12}(z, t_{C_2}t_{C_2}, \Delta)$ in equation (S24), where the echo becomes emissive. Therefore, π - 3π control pulse sequence is valid for a single rephasing scheme as shown in refs. [18]. Thus, the controlled AFC echoes with the π - π control pulse sequence [8,9] results in an absorptive echo [25]. The observation of the controlled AFC is due to coherence leakage by spatial Gaussian distribution of laser light [20].

References

24. Mitsunaga, M. and Uesugi, N. 248 bit optical storage inEu3p: YAIO3 by accumulated photon echoes. *Opt. Lett.* **15**, 195–197 (1990).
25. Ham, B. S. Analysis of optical locking applied for rephasing halt in photon echoes. *J. Opt. Soc. Am. B* **28**, 775 (2011).
26. Azadeh, Sjaarda Cornish, M. C. Babbitt, W. R. and Tsang, L. Efficient photon echoes in optically thick media. *Phys. Rev. A* **57**, 4662 (1998).
27. Ruggiero, J. Le Gouët, J.-L. Simon, C. and Chanelière, T. Why the two-pulse photon echo is not a good quantum memory protocol. *Phys. Rev. A* **79**, 053851 (2009).

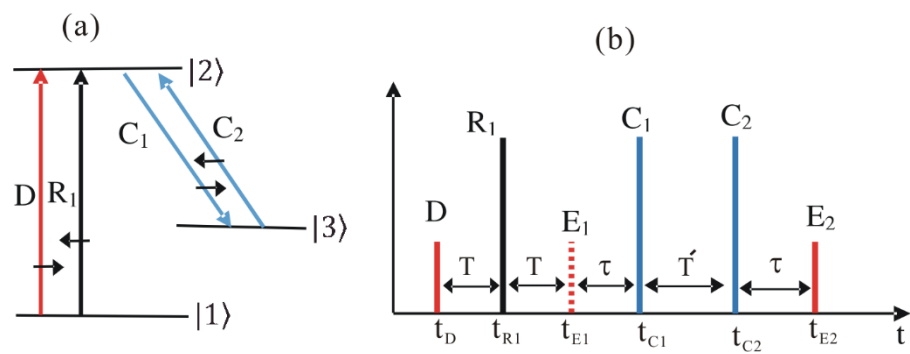


Fig. S1. (a) Schematic of backward single rephasing photon echoes in a three-level system. (b) Pulse sequence for (a). The t_j is the arrival time of pulse j .